Numerical analysis of the cliff failure occurred at St. Eutizio Abbey during the 2016 Central Italy seismic sequence

Somma Fausto[1], Cortellesi Benedetta[2], Pagliaroli Alessandro[3], Tommasi Paolo[4], Lanzo Giuseppe[5]

[1] *Geotechnical Engineer, Former Researcher at Dpt. of Structures for Engineering and Architecture (DiSt), University of Naples Federico II: fausto.somma@unina.it*

[2] *PhD Student, Dpt. of Structural and Geotechnical Engineering, Sapienza University of Rome, email: benedetta.cortellesi@uniroma1.it*

[3] *Full Professor, Dpt. of Engineering and Geology, University of Chieti Pescara, email: alessandro.pagliaroli@unich.it*

[4] *Senior Researcher, Institute of Environmental Geology and Geoengineering (IGAG), National Research Council (CNR), email: paolo.tommasi@cnr.it*

[5] *Full Professor, Dpt. of Structural and Geotechnical Engineering, Sapienza University of Rome, email: giuseppe.lanzo@uniroma1.it*

ABSTRACT

Among the religious monuments that were severely damaged by the 2016-17 Central Italy seismic sequence, one of the most important is the St. Eutizio Abbey (Preci, Umbria Region). The Abbey rises at the foot of a 25-m-high sub-vertical cliff delimiting a wedge-shaped travertine spur, on top of which a cemetery and the bell tower of the Abbey are located. The October 30th main shock caused the failure of the cliff and the successive collapse of the bell tower. The aim of this study is to investigate the structural and geotechnical factors controlling these failures. A geotechnical slope model was developed using LiDAR, borehole data, and laboratory tests. Bi-dimensional stress-strain dynamic analyses (linear and non-linear elasto-plastic) were conducted to evaluate how stratigraphy and topography modified the seismic motion, analyse the state of stress induced by the seismic events in the travertine spur, and hence the triggering of failure phenomena both in the rock and in the rock-interacting structures. Additionally, a three-dimensional analysis to get preliminary information on the potential effects of soil–structure interaction on the dynamic behaviour of the tower was performed.

Keywords: Seismic response analysis, Numerical modelling, Seismic Risk Assessment, 2016-2017 Central Italy seismic sequence, slope instability, soil-structure interaction

INTRODUCTION

The preservation of cultural heritage has been a matter of utmost importance for many European countries since the early 19th century. In recent years, it has become evident that effective intervention poses a complex challenge that requires balancing multiple scientific disciplines as the structural stability of monuments can be endangered by various hazards, including geotechnical issues and earthquakes. The 2016 Central Italy seismic sequence caused extensive damage to cultural heritage sites, and in several cases the occurrence of major seismic events within a short time span ultimately led to their collapse. A striking example is the bell tower of St. Eutizio Abbey (Preci, Umbria region), which collapsed following the failure of the steep cliff on which it had been built.
Within this context, this paper presents a research work carried out within the national project (PRIN) entitled: “GIANO – Geo-Risks Assessment and Mitigation for the Protection of Cultural Heritage" funded in 2020. This study combines geological surveys, borehole investigations, laboratory testing and advanced numerical modelling to assess the dynamic cliff response and the structural vulnerability of the bell tower. The work aims to provide new insights into the failure processes that occurred during the

2016 seismic sequence, by analysing both stratigraphic and topographic effects on ground motion affecting the area as well as the role of pre-existing fractures on the dynamic behaviour of the cliff.

ST. EUTIZIO ABBEY: HYSTORY AND EVENTS

The St. Eutizio Abbey represents one of the most relevant medieval religious complexes in the Central Italy, as it is traditionally identified as the place of origin of the Benedictine monastic order. The complex is located close to the village of Preci, 60 km to the south-west of Perugia, in the Umbria region (Figure 1, left). The monastic complex, consisting of a church and various edifices, is built at the foot of a rock spur (Figure 2, left), excepting for the bell tower, rising at the edge of the rock spur together with the cemetery. At the end of the 19th century, the site was affected by several seismic events that caused numerous and devastating damages to the entire complex. Between August and October 2016, three major earthquakes occurred in Central Italy (Figure 1, right), generated by the activity of normal faults located along the Apennines chain. The first mainshock took place on August 24th 2016 (Mw=6.0), followed by two further events on October 26th (Mw=5.9) and October 30th (Mw=6.6). The August 24th event, whose epicentre was located 23 km from the site of interest, caused limited damage. The seismic event of October 30th, with an epicentre only 5 km from the Abbey, triggered a failure of the cliff leading to the collapse of the bell tower built at its edge and of large part of the funerary shrines built behind the edge itself (Figure 2, right).

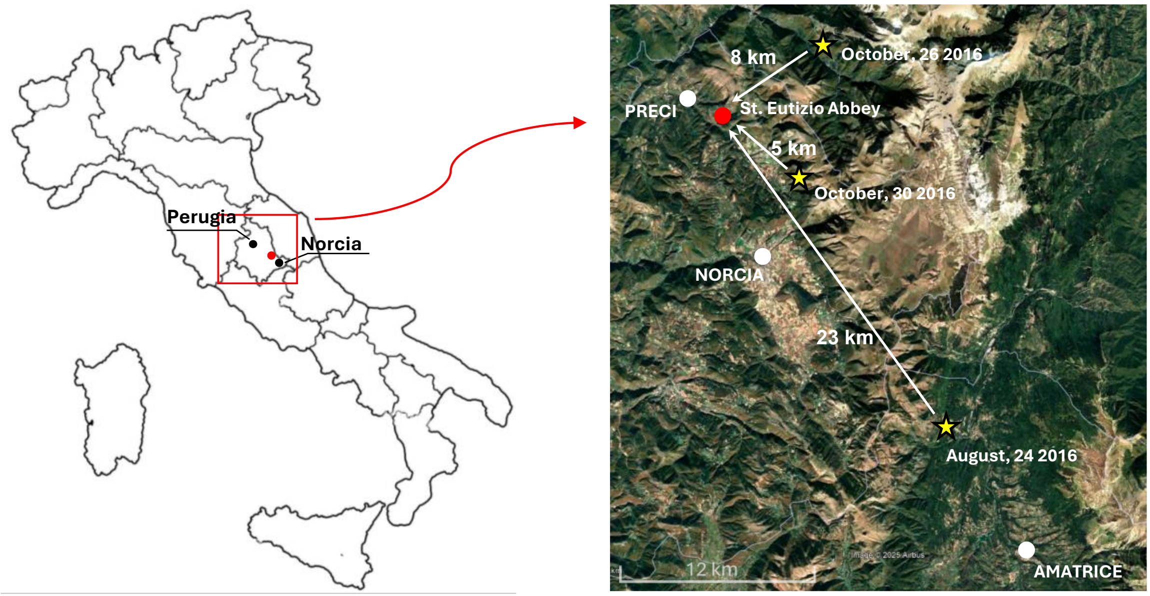

***Figure 1**: Location of the St. Eutizio Abbey (left) and epicenters of three 2016 seismic events (right)*

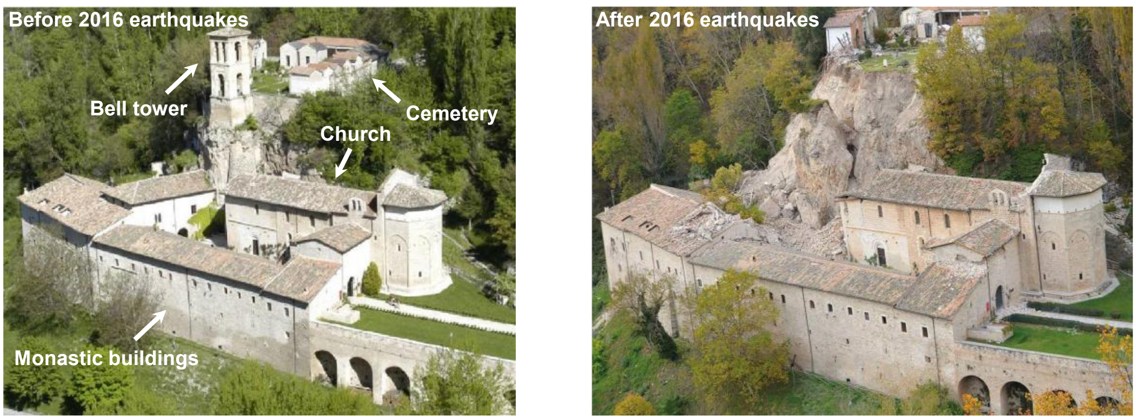

***Figure 2**: The St. Eutizio Abbey: before (left) and after (right) the 2016 earthquakes*

GEOLOGICAL SETTING AND GEOTECHNICAL INVESTIGATIONS

The geological setting of the area is the result of an older compressive tectonic phase and a successive extensional phase, still active. In this respect, the Abbey rises along a segment of the active SW dipping Norcia Fault, considered to be a potential source of Mw 6.5-7 earthquakes (Maceroni et al., 2022) and is only 5 km distant from the epicentre of the Mw 6.5 earthquake of October 30th 2016, linked to the SW dipping Mt. Vettore-Mt. Bove fault, outcropping 11 km east to the Abbey.

The monastery is built at the foot of a spur with a flat top formed by a travertine deposit (calcareous tufa). The spur is bounded on the western side by a narrow incision and on the southern side by an up-to-23-m high steep cliff overlooking the Abbey. At the cliff edge, the bell tower was founded on a prominent rock prism, whilst a cemetery rises on the spur top. Conversely, on the northern and eastern sides the spur pinches out and joins up with continuity to the valley flank. The travertine deposit consists of a thick highly porous rock core sandwiched by an upper and bottom layer of uncemented carbonate sands and gravels.

The travertine deposit overlies the Mesozoic-Cenozoic substratum, which in the NE part of the monastery is formed by micritic limestones (*Maiolica Formation*, lower Cretaceous) and in the SW part by thin alternating layers of limestone and sheared scaly clays (*Marne a Fucoidi Formation*, middle Cretaceous). The geological units of the substratum form the limb of a small syncline. According to Maceroni et al. (2022), at the western limit of the Abbey a reverse thrust dipping towards ENE puts in contact the Cretaceous formations with the younger shale formation of *Scaglia Cinerea* (Paleogene).

Between the travertine deposit and the substratum, a very heterogeneous deposit (likely a slope debris) is interposed. It is formed by a mixture of clay, silt, sand and fine angular gravel in variable proportions. In the outermost part of the rock spur, gaping subvertical fractures roughly parallel to the cliff face were observed, both in the horizontal borehole BH (Figure 4) and on the cliff. Fractures are very widely spaced (at least a couple of meters) and were likely produced by the state of stress acting at the spur margin. In the vertical borehole DH, drilled at the centre of the spur, dissolution cavities have also been encountered, which are also visible on the western face of the rock cliff.

Investigation campaigns

Several campaigns of subsurface investigations were conducted from 1999 to 2024 for slope stabilization (Preci municipality in 1999), reconstruction after the 2016-2017 seismic sequence (Umbria Region in 2018, Spoleto archiepiscopal office in 2019 and 2022) and in the framework of two research projects (Sapienza University of Rome in 2022 and "GIANO" National Research Project PRIN in 2023). Ten boreholes were core-drilled (Figure 2). Seven are in the monastery area: S1, S2, S3, S4 in 2019; B1 and B2 in 2022; BH3 (sub-horizontal) in 2023. Three are in the cemetery area, on top of the rock spur: S0 in 1999, B3 and DH in 2022). The sub-horizontal BH3 borehole was drilled at the foot of the rock spur, close to the vertical B1 and B2 boreholes. Groundwater was not detected within the investigated stratigraphic sequence (Figure 4), so groundwater table was not included in the numerical analysis.

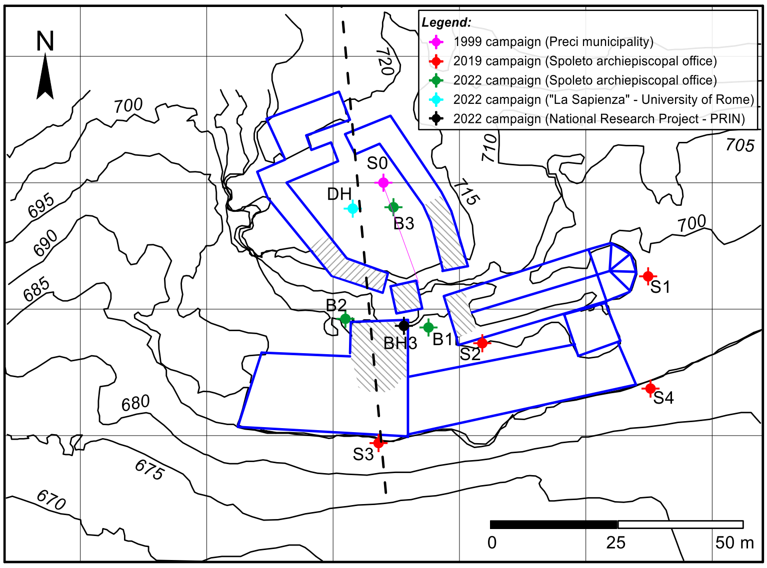

***Figure 3**: Location of boreholes. Hatched areas indicate parts of the building failed during the earthquakes. The dashed line is the trace of the profile in Figure 3*

During all vertical drillings, except for S0, SPTs were carried out. In the DH borehole drilled at the top of the cliff a downhole was carried out to measure seismic velocities of the different lithotypes. Logs of stratigraphy N_{SPT} values and S-wave velocity are shown in Figure 4. Ultrasonic pulse laboratory tests were also conducted on travertine core samples to better appraise results of the down-hole test.
There is an overall good agreement between the S- and P- wave velocity measures and borehole stratigraphic logs with only slight differences between the depth of the transition between sand and travertine at shallower depths. In situ and laboratory measurements of elastic wave velocities of the travertine provided comparable and relatively high values (on average V_P ~ 3300 m/s and V_S ~ 1600 m/s). This result clearly indicates that the travertine is cemented and that the largely spaced fractures that cross the rock mass scarcely affect the stiffness measured in-situ.

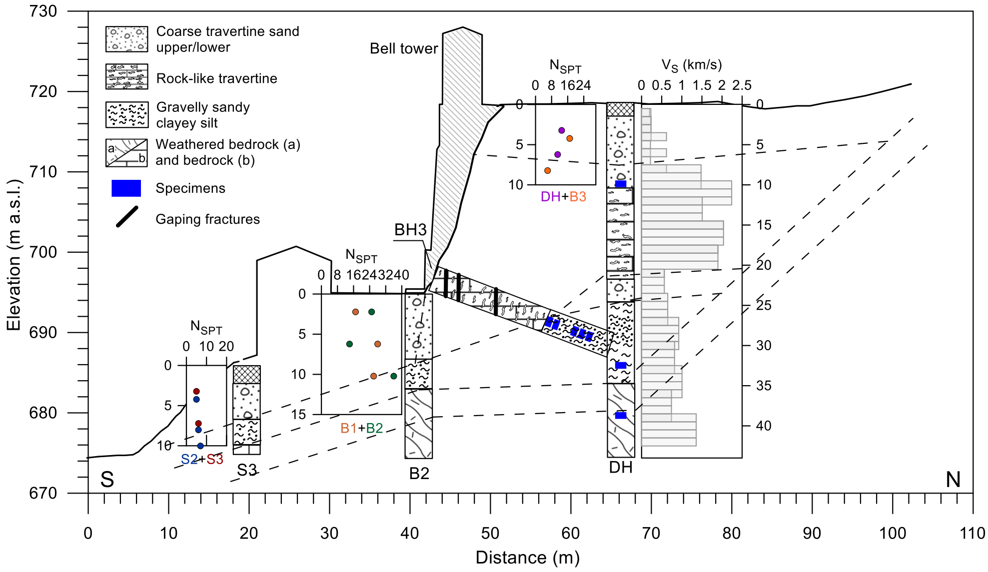

***Figure 4**: N-S profile (trace in Figure 2) reporting sample depths, borehole stratigraphy and logs of N_{SPT} value, and shear wave velocities*

Conversely, the coarse sand sandwiching travertines display much lower velocities (V_P ~ 500 m/s, and V_S ~ 225 m/s for the upper sands and V_P ~ 1250 m/s and V_S ~ 600 m/s for lower sands). The transition between the lower sands and the gravelly sandy clayey silt is highlighted by an increase in velocity (V_S passes from 500 to 850 m/s). Finally, velocity sharply increases in the bedrock (V_P ~ 3700, V_S ~ 1350 m/s) (alternating layers of stiff clay shale and limestone), which is softened and weathered at its top.
Values of N_{SPT} indicate that the carbonate sands are loose, especially those overlying the travertine. N_{SPT} values of the sands encountered by boreholes B1+B2 below the foot of the travertine cliff are slightly higher, probably due to the higher lithostatic stress exerted in the past by the travertine spur before its retreat until the present position. The scarce packing results also in low bulk unit weight (γ=16 kN/m^3) and low shear strength (ϕ'= 31° from direct shear tests), determined in the 2022 campaign. For the slope debris interposed between the travertine deposit and the bedrock, tests conducted in the same campaign provided values of γ and water content, w_n, of 19.8 kN/m^3 and 23.4% respectively, and effective cohesion and shear strength angle from direct shear tests of 30 kPa and 30°, respectively.
The rock-like travertine has a porosity in the range 24-36%, which corresponds to a unit bulk weight in the range 17-19 kN/m^3. The uniaxial strength of the travertine measured in the 1999 campaign, probably referring to the weakest horizons, varies between 3.5 and 7.5 MPa.

NUMERICAL ANALYSIS

A two-dimensional finite element model was set up using PLAXIS 2D (v.2024.2, Bentley Systems, Inc.) to analyse the mechanisms that were potentially responsible for the cliff collapse and the associated failure of the bell tower during the 2016 Central Italy seismic sequence. The model domain spans 450 meters in width and 150 meters in depth, incorporating a stratigraphic profile reconstructed from borehole investigations and geophysical surveys, as detailed in prior sections. The structural load imposed by the bell tower was schematized through an equivalent uniform vertical pressure of approximately 50 kPa. The foundation was explicitly modelled to account for seismic-induced kinematic amplification at the cliff edge. The finite element mesh consists of 18,462 15-node triangular elements, providing a spatial resolution sufficient to accurately model both the transient dynamic behaviour and the localization of strain and displacement patterns. In particular, the element size satisfies the criterion for maximum frequency propagation proposed by Kuhlemeyer and Lysmer (1973), ensuring accurate seismic wave transmission across the model domain. To minimize artificial boundary reflections, a compliant (viscous) boundary condition was applied at the model base, while free-field conditions were imposed along the lateral boundaries to permit realistic lateral propagation of seismic waves. The stratigraphy of the model comprises the following geotechnical units from top to bottom (Figure 5): alluvial deposits (A), upper travertine sand (ST1), massive rock-like travertine (T), lower travertine sand (ST2), the colluvial gravels and sands with silty-clayey matrix (C) and the bedrock (B), with its weathered top layer (WB). Furthermore, the bell tower foundation was considered as a distinct material (F). The vertical gaping joint located a few metres behind the cliff face (J) was explicitly represented in the numerical model using a PLAXIS interface element. Thus, the joint was implemented as a thin zero-thickness interface to account for its reduced shear strength, allowing to investigate its influence on the deformation patterns and failure mechanisms of the slope.

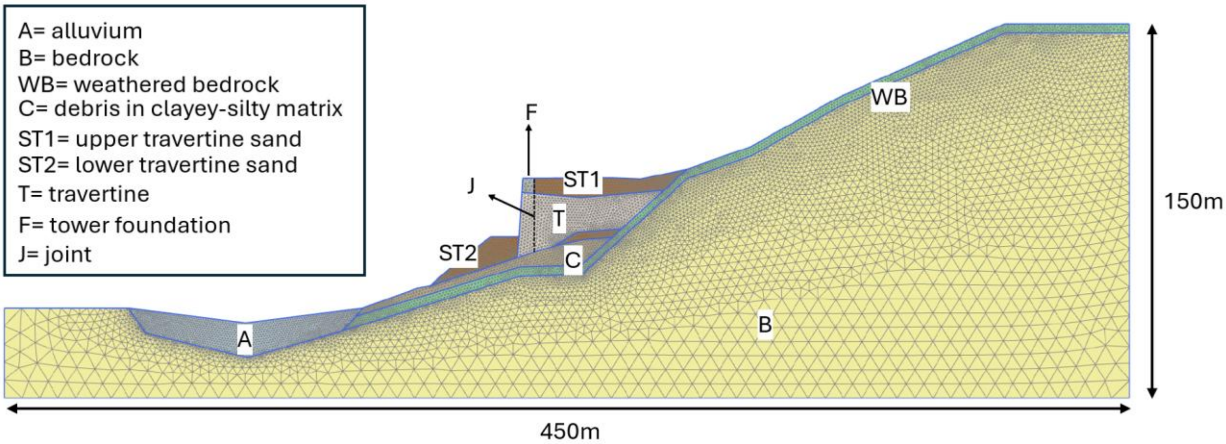

Figure 5. *Two-dimensional model of the slope used in the numerical analyses with computational mesh and geotechnical units*

Different constitutive models were selected to represent the mechanical behaviour of the various geotechnical units, based on their lithological characteristics and the anticipated levels of shear strain during seismic excitation. The bedrock (B) and its weathered top layer (WB) were modelled as purely visco-elastic materials, as they were expected to remain within the elastic range due to their high stiffness and the limited strain demand imposed by the seismic loading. Similarly, the alluvial deposit (A), located at the toe of the slope and far from the failure zone, was also assigned a visco-elastic behaviour, given its limited influence on the dynamic response of the cliff (Table 1). In contrast, the upper and lower travertine sands (ST1 and ST2) and the colluvial deposit (C) were modelled using the Hardening Soil model with small-strain stiffness (HS_{ss}). This advanced constitutive formulation was adopted to capture the stress- and strain-dependent shear stiffness reduction and hysteretic damping behaviour under cyclic loading, which are critical for accurately representing the seismic response of these more deformable soil units. The massive travertine unit (T), the foundation base layer (F), and the joint (J) were all modelled using an elasto-plastic Mohr–Coulomb constitutive law, which was considered an acceptable compromise for simulating a stiff, brittle rock-like material with a simplified yet effective failure envelope. The open fracture (J) was explicitly modelled using interface elements embedded within the surrounding travertine rock mass. The joint material was assigned null tensile strength and cohesion (i.e., no bonding between the joint surfaces due to the gap), while the friction angle was set to 20°, corresponding to a reduced friction angle of the travertine, to simulate the diminished contact area between the joint surfaces due to gaping. The dynamic properties assigned to each material model, including stiffness parameters, damping coefficient, and strength parameters, are summarized in Tables 1 and 2.

Table 1. *Mechanical parameters of first set of visco-plastic and Mohr-Coulomb elasto-plastic materials*

Unit [-]	γ [kN/m^3]	v [-]	V_s [m/s]	D_0 [%]	ϕ' [-]	c' [kPa]	f_t [kPa]
A	18.00	0.20	150	1.00	-	-	-
T	17.50	0.35	1600	0.70	40	2300	2700
WB	20.30	0.48	742	0.70	-	-	-
B	20.30	0.42	1358	0.50	-	-	-
F	16.00	0.20	1200	1.00	41	447	400
J	17.50	0.35	507	0.70	20	0	0

γ=unit weight, v= Poisson's ratio V_s= shear wave velocity, D_0= Rayleigh damping, ϕ'= friction angle, c'=effective cohesion, f_t=tensile reistance

Table 2*. Mechanical parameters of the materials with HSsmall model*

Unit [-]	γ [kN/m^3]	v_{ur} [-]	$E_{50,ref}$ [MPa]	$E_{oed,ref}$ [MPa]	$E_{ur,ref}$ [MPa]	$G_{0,ref}$ [MPa]	$\gamma_{0.7}$ [-]	m [-]	ϕ' [°]	c' [kPa]
ST1	17.3	0.2	14.17	14.17	42.5	88.54	1.1×10^{-4}	0.1	35	5
ST2	17.3	0.2	99.32	99.32	298.0	620.80	1.1×10^{-4}	0.1	42	10
C	19.9	0.2	237.00	237.00	710.9	1481.00	1.86×10^{-4}	0.1	27	26

$E_{50,ref}$ =deviatoric ref. mod., $E_{oed,ref}$ =compression ref.mod., $E_{ur,ref}$ =load-unload ref. mod., $G_{0,ref}$=ref. shear modulus, $\gamma_{0.7}$=Ref. shear strain, m= dependence of stress level

Input motions

Two acceleration time histories of two of the three major shocks of the 2016 Central Italy seismic sequence, recorded at stations that are representative of epicentral distance and geology of the site, were selected. The first input corresponds to the August 24th earthquake (Mw 6.0) and the October 30th (the strongest event of the sequence, Mw 6.6). The former ground motion was recorded at the Monte Fiegni Fiastra station (station code: IT.MNF), located approximately 40.3 km from the epicentre, at outcropping rock conditions (V_{s30}=1062 m/s), with a recorded peak ground acceleration (PGA) of 0.044g (NS component). Since the Sant'Eutizio Abbey lies at a closer distance to the epicentre (22.16 km), the recorded time history was scaled to 0.07g using the Ground Motion Prediction Equation (GMPE) proposed by Bindi et al. (2011), in order to more realistically reflect the expected shaking intensity at the site. The latter is a near-field accelerometric record acquired by a temporary seismic station installed in the town of Preci (station code: PRE), located on marly limestones with V_{s30}= 923 m/s, with a recorded peak ground acceleration (PGA) of 0.31g (NS component) and situated close to the study area (2.7 km). For both seismic events, two input components were applied at the base of the model: the horizontal (NS) component, aligned with the north–south orientation of the modelled cross-section, and the vertical (Z) component. The application of both components represents more accurately the seismic demand imposed on the slope and the bell tower foundation, particularly considering the near-fault effects and the potential for vertical motion amplification at the cliff edge. Figure 6 and Table 3 summarize the principal characteristics of the selected ground motion signals.

Table 3. *Characteristics of dynamic input motion (horizontal NS component)*

Signal	T_d *[s]*	T_m *[s]*	a_{max} *[g]*	*AI* *[m/s]*	$T_{5\text{-}95}$ *[s]*
24 August	0.26	0.36	0.07	0.039	10.91
30 October	0.14	0.24	0.31	0.918	11.16

T_d = predominant period, T_m = mean period, *AI* = Arias intensity, $T_{5\text{-}95}$ = significant duration

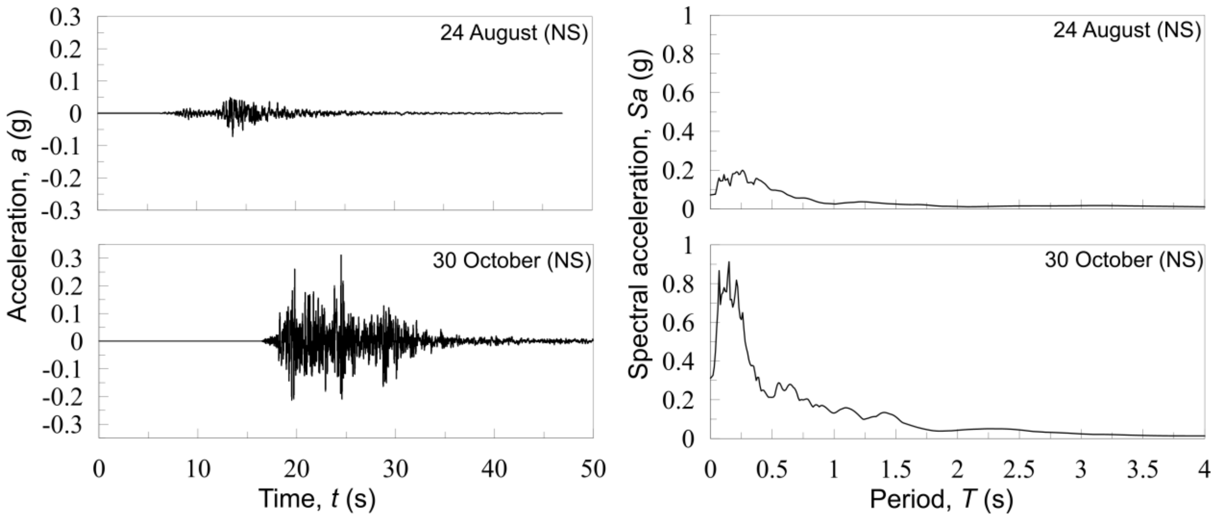

Figure 6. *(left) Seismic input motions considered in the present study (horizontal NS components) and corresponding spectral acceleration (right)*

RESULTS AND DISCUSSION

The results of the dynamic analyses offer critical insights into the seismic response of the travertine spur overlooking the St. Eutizio Abbey. A pronounced amplification of ground motion is observed at the edge of the cliff, where peak ground acceleration (PGA) reaches approximately 0.3 g and 0.7–0.8 g for the August 24th and the October 30th seismic events, respectively (Figure 7).

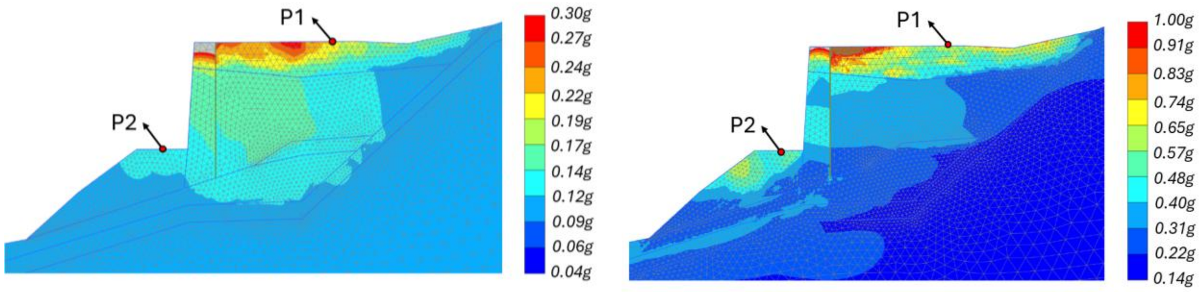

Figure 7. *Contours of PGA for August 24 (left) and October 30 (right) earthquakes*

A clear amplification of peak accelerations is also observed close to the bell tower foundation, representing a strong impedance contrast between the stiff foundation layer and the adjacent softer sand. Amplification is likely enhanced by a topographic amplification effect induced by the cliff geometry. Moving from the cliff edge inward, acceleration systematically reduces. It is worth noting that the maximum accelerations are consistently recorded at the top of the rock spur (see for example monitoring point P1), highlighting the role of topographic and stratigraphic amplification (i.e., the relevant impedance contrast between ST1 sandy layer and the underlying unit T). In contrast, the area corresponding to the main edifices of the abbey (monitoring point P2) exhibits lower motion, suggesting a spatial variability in seismic demand that has important implications for site-specific seismic hazard and structural vulnerability assessments (Figure 8).
In the numerical model, the cliff failure is reasonably reproduced by the detachment and toppling of the travertine prism under the October 30 seismic loading (Figure 9). Conversely, during the August 24th event, no significant plastic residual displacements were observed, in agreement with field evidence. As shown in Figure 9, the pre-existing open joint is instrumental for the complete separation of the marginal prisms/columns of the travertine spur from the rock mass behind. This is consistent with the collapse pattern documented during post-earthquake surveys. The final plastic horizontal displacements predicted by the model are in the order of centimeters, i.e., smaller than those observed in the field, where the toppled travertine prism moved few meters. This discrepancy suggests that the numerical analyses effectively capture the initiation phase of the failure process — that is, the conditions leading

to instability, detachment and rotation — but not the full kinematic development of the toppling of the rock prism, which would require more advanced post-failure simulations.

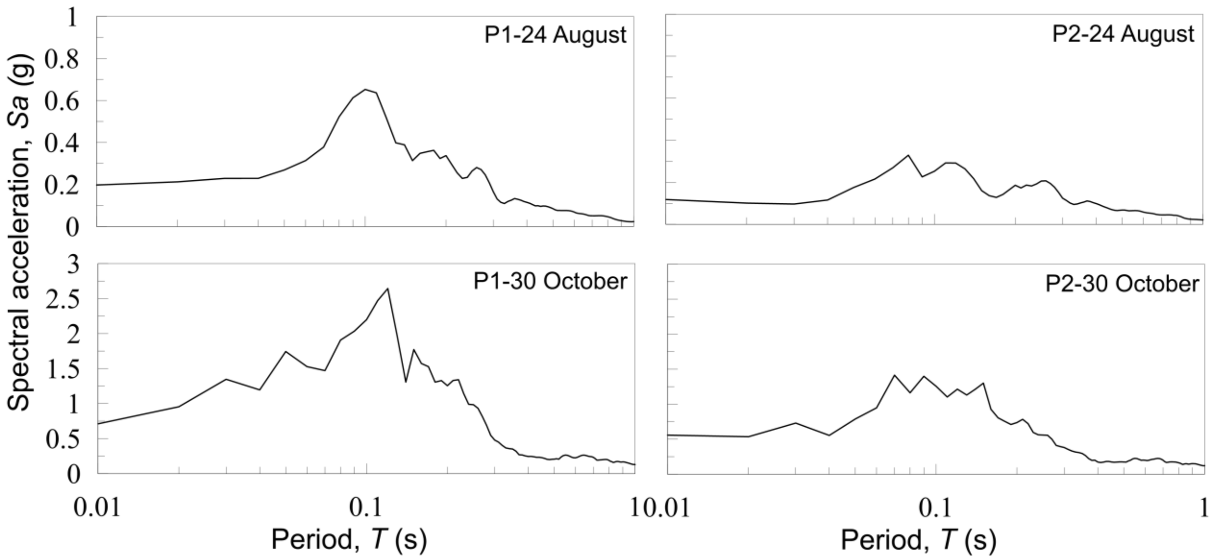

Figure 8. *Acceleration response spectra at P1 (left) and P2 (right) reference points*

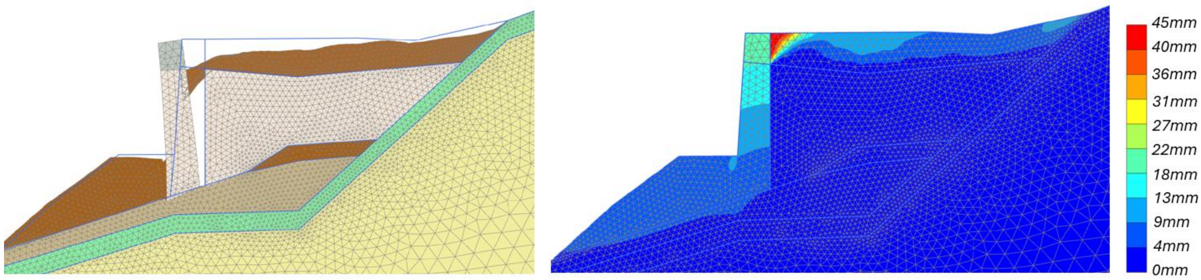

Figure 9. Numerical simulation for October 30th event: *(left) deformed mesh showing the failure mechanism of the travertine cliff, characterized by detachment and rotational collapse of the marginal prism (right) contour of permanent total displacements*

Simulations performed without explicitly modelling the gaping rock joint still show significant dynamic amplification effects; however, no signs of large-scale instability or permanent displacements are observed consistent with the findings reported by Lanzo et al. (2024). This result suggests that the travertine rock mass remains globally stable under seismic loading, unless pre-existing open discontinuities are considered. Discontinuities allow the spur margin to be kinematically independent from the inner portion of the rock mass, which behaves as a virtually monolithic body, due to the absence of systematic joints that, conversely, typically feature most of the rock masses.

Insight into the seismic response of bell Tower

As previously mentioned, the bell tower was not explicitly modelled in the 2D dynamic analyses. Only its structural load was applied as a uniform vertical pressure on the foundation base, which was embedded in the travertine. To gain insight into the structural behaviour of the tower, a detailed three-dimensional geometric survey was conducted (Capaldini, 2022, pers. comm.), and the resulting point cloud was used to develop an accurate 3D CAD model of the bell tower (Figure 10). This model was then imported into PLAXIS 3D, where a simplified dynamic analysis was performed to estimate its fundamental vibration period using a sinesweep base excitation.

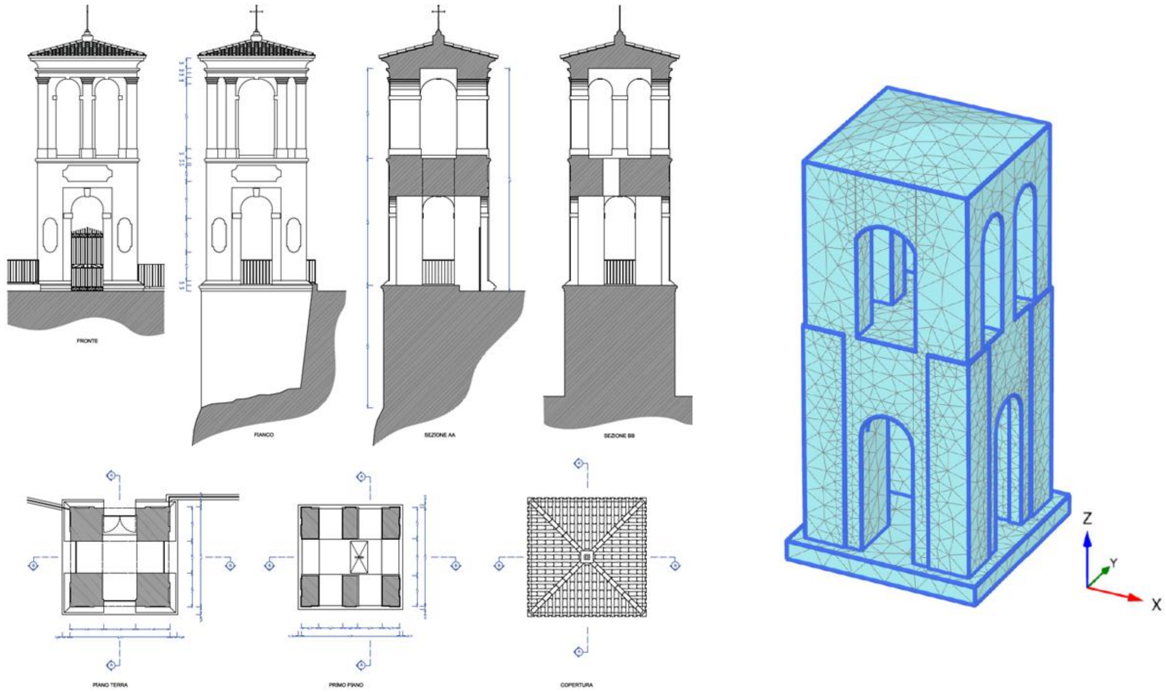

Figure 10. *Geometric survey of the bell tower (left) and corresponding 3D model implemented in PLAXIS 3D (right)*

The masonry was modelled with an elasto-plastic Mohr-Coulomb model assigning both high-quality (Tower A) and poor-quality (Tower B) mechanical properties, based on the indicative ranges provided by the Italian Building Code (NTC, 2018) (Table 4). Furthermore, the fundamental vibration periods were found by evaluating the amplification function between the base and the top of the tower (see T_x and T_y in Table 4).

Table 4. *Mechanical parameters adopted for the masonry material of the tower*

Tower Type	γ *[kN/m3]*	v *[-]*	E *[MPa]*	Φ *[°]*	c' *[kPa]*	f_t *[kPa]*	T_x *[s]*	T_y *[s]*
A	16.00	0.20	1200	42	447	400	0.24	0.26
B	16.00	0.20	900	30	50	500	0.27	0.29

Finally, the potential effects of soil–structure interaction (SSI) on the dynamic behaviour of the tower were assessed through the formulation of De Silva et al. (2024). The results indicate that SSI effects were negligible in terms of both period elongation and additional damping. This finding is consistent with the high stiffness of the rock-like travertine layer on which the tower is founded, which behaves essentially as a rigid base under seismic loading. Considering the sharp amplification of seismic motion at the crest of the cliff, the tower was likely subjected to very high acceleration demands, particularly under the October 30th event. This effect would have been critical especially in the case of low-quality masonry (Type B parameters), where the capacity of the structure to resist inertial loads would have been significantly lower. Moreover, the estimated fundamental vibration periods of the tower in the X-direction (ranging from 0.24 s to 0.27 s) fall within the portion of the response spectrum that is typically associated to high spectral accelerations, which in this case exceed 1g. This suggests that a resonance phenomenon between the fundamental frequency of the structure and the dominant frequencies of the input ground motion likely contributed to the dynamic vulnerability of the tower.

CONCLUSIONS

This study investigated the geotechnical and structural response of the travertine cliff and the bell tower of the St. Eutizio Abbey, collapsed during the October 30th 2016 earthquake in Central Italy. Through 2D dynamic finite element analyses calibrated on detailed geotechnical and geological data, the triggering mechanism of the cliff failure was effectively reproduced, particularly the detachment and toppling of the marginal rock prism, delimited by pre-existing gaping fractures. Seismic motion was found to be significantly amplified at the top and edge of the travertine spur with peak ground accelerations exceeding 0.7–0.8g and spectral accelerations of about 2.5g in the period range 0.1-0.2 s for the October 30^{th} event. This was due to the combined effects of topography and stratigraphic impedance contrasts. The 3D structural analysis of the bell tower, supported by a high-resolution geometric model, showed that its fundamental vibration period lies within a range (0.24–0.29 s) where spectral acceleration demand is high. Soil-structure interaction effects were found to be negligible due to the rigidity of the travertine bedrock. However, the dynamic amplification observed at the plateau edge suggests that the tower was subjected to extremely high inertial forces that likely exceeded its structural capacity, particularly under the assumption of degraded material properties. The findings of this work emphasize the importance of integrating geological, geotechnical, and structural data to understand failure mechanisms in heritage sites located in seismically active areas. In the context of reconstruction efforts, these results can support the definition of risk mitigation strategies for the reconstruction of the bell tower. It becomes essential to identify if other open fractures are present in the travertine body and to map them. Eventually, reinforcement techniques could be conveniently applied where necessary (e.g., bolting with fully grouted passive bars) to restore global slope stability and prevent future detachments.

ACKNOWLEDGEMENTS

The Authors acknowledge the kind assistance of the municipality of Preci (PG) and its mayor, Massimo Messi, and the Archdiocese of Spoleto-Norcia, in the person of Monsignor Ceccarelli, for access to the Abbey and to documentation of previous geological and geophysical investigations. The assistance of Eng. Giampaolo Capaldini in retrieving this documentation is also gratefully acknowledged.

This work has been supported by the project "GIANO – Geo-Risks Assessment and Mitigation for the Protection of Cultural Heritage" funded by the MIUR *Progetti di Ricerca di Rilevante Interesse Nazionale* (PRIN) Bando 2020. P. Tommasi benefited from CNR funding (IGAG Project "Static and dynamic analysis of rock slopes").

REFERENCES

Bentley Systems, Inc. (2024). PLAXIS 2D and 3D (Version 2024.2) [Computer software]. Bentley Systems, Inc., Exton, PA, USA

Bindi D., Pacor F., Luzi L., Puglia R., Massa M., Ameri G., Paolucci R. (2011). Ground motion prediction equations derived from the Italian strong motion database. Bullettin of Earthquake Engineering 9, 1899-1920, https://doi.org/10.1007/s10518-011-9313-z

Capaldini G., Fabrizio Bonucci F. (2022). Architectural survey of the existing condition of the bell tower. Studio Associato di Ingegneria Capaldini (in Italian)

De Silva, F., Silvestri, F. (2024). Derivation, Validation, and Web Application of Dimensionless Analytical Solutions for Equivalent Period and Damping Ratio of Soil-Foundation-Structure Systems. Journal of Geotechnical and Geoenvironmental Engineering, 151(6), https://doi.org/10.1061/JGGEFK.GTENG-12927

Kuhlemeyer, R.L., & Lysmer, J., (1973). Finite element method accuracy for wave propagation problems. J. Soil Mech. Found. Div, 99, 421-427.

Lanzo G., Tommasi P., Cercato M., De Donno G. (2024). Site characterization and seismic response analysis of the cliff overlooking the St. Eutizio Abbey, Central Italy. GeoMontreal 2024, GEOM711_0729113342, 15-18 September 2024, Montreal.

Maceroni D., Falcucci E., Gori S., Motti A., Moro M., Saroli M., Dixit Dominus G., Doumaz F., Galadini F. (2022). Assessing active and capable faulting as best practice for post-earthquake reconstruction activities: the Sant'Eutizio Abbey case study, in the epicentrali area of the 2016 central Italy seismic sequence. Annals of Geophysics, 65 (1), doi: 10.4401/ag-8793.

NTC (2018) Norme Tecniche per le Costruzioni. DM 17/1/2018, Italian Ministry of Infrastructure and Transportation, G.U. n. 42, 20 February 2018, Rome, Italy (in Italian)